The calculated electronic and magnetic structure of martensite iron nitrides

1993 J. Phys.: Condens. Matter 5 1411

(http://iopscience.iop.org/0953-8984/5/9/025)

J. Phys.: Condens. Matter 5 (1993) 1411–1418. Printed in the UK

The calculated electronic and magnetic structure of martensite iron nitrides

Zhi-qiang Li†

CCAST (World Laboratory), PO Box 8730, Beijing 100080, People's Republic of China, and Institute of Physics, Academia Sinica, Beijing 100080, People's Republic of China

Received 25 November 1992, in final form 4 January 1993

Abstract. The electronic structure and local magnetic moment of BCT-FeN compounds were calculated by the first-principles self-consistent cluster method. For the α'-martensite, we found that the magnetic moment of the first-neighbour Fe atoms of N was reduced while that of the second-neighbour Fe atoms was increased compared with those of pure BCC-iron; this was attributed to the concomitant effects of p–d interactions and tetragonal elongation of BCT-FeN, and was in good agreement with experiment. For the $Fe_{16}N_2$ structure, the calculated average magnetic moment is smaller than that of experiment.

1. Introduction

In 1972, Kim and Takahashi [1] discovered that iron films evaporated in a nitrogen atmosphere exhibit a highly saturated magnetic flux density $B_s \approx 2.8$ T, while for pure iron $B_s \approx 2.2$ T. They concluded that this is due to the formation of a ferromagnetic compound $Fe_{16}N_2$ in the films. According to their rationalization, the average magnetic moment per iron atom in the $Fe_{16}N_2$ may be about $3\mu_B$. Many investigations have been carried out to study the magnetic properties of Fe–N compounds since then [2–8]. However, because it is very difficult to manufacture single-phase $Fe_{16}N_2$, its high magnetization was only debated until the single-phase $Fe_{16}N_2$ films were produced by Sugita *et al* [8] by molecular beam epitaxial (MBE) growth which confirmed the high magnetization of $Fe_{16}N_2$.

The structure of $Fe_{16}N_2$ is BCT, which was first proposed by Jack [9] in 1952, comprising $2 \times 2 \times 2$ unit cells of the BCC Fe lattice, see figure 1. This means that it can be described as an α''-martensite with an ordered distribution of nitrogen atoms in the deformed octahedral interstices, while in the α'-martensite, the nitrogen atoms occupy the octahedral interstices with a disordered distribution. In $Fe_{16}N_2$ structure, there are three inequivalent Fe sites (Fe(1), Fe(2) and Fe(3)) according to their distances from the N atom.

$Fe_{16}N_2$ films can be made by evaporation [1], ion implantation [4] and MBE [7, 8]. The first and second methods can only produce the mixed-phase samples. The single-phase $Fe_{16}N_2$ films were made by MBE growth on Fe(100)/InGaAs(001) substrate [8].

† Permanent and mailing address: Department of Physics, Tsinghua University, Beijing 100084, People's Republic of China.

0953-8984/93/091411+08$07.50

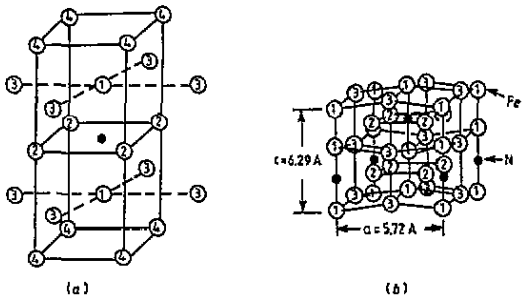

Figure 1. The structure of α'-martensite. (*b*) The structure of α''-$Fe_{16}N_2$. Numbers in the circles are the order of distance from the central N.

Moriya *et al* [2], and Mitsuoka *et al* [3] studied the magnetic properties of α'-FeN films. The Mössbauer spectrum consisted of the components of Fe(1), Fe(2), Fe(3) and other Fe sites in the structure, see figure 2. The hyperfine fields of Fe(1) decrease relative to α-Fe, but those of Fe(2) increase. The fourth-nearest-neighbour Fe sites from N are not affected by the N atom, indicating that the effect of N atoms is relatively local.

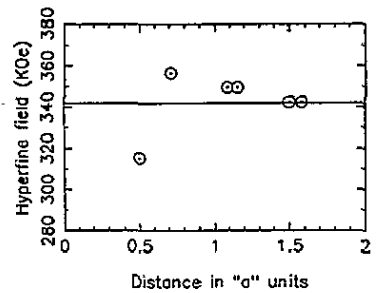

Figure 2. The hyperfine fields for the different sites of iron atoms in α'-martensite structure according to the distances from the N atom. From [2].

Many studies on $Fe_{16}N_2$ films have also been performed, see table 1. Kim and Takahashi first obtained $B_s \approx 2.8$ T and their Mössbauer spectrum contained only two components; this does not correspond to the actual structure of $Fe_{16}N_2$. Nakajima *et al* have found $B_s \approx 2.66$ T in ion-implanted $Fe_{16}N_2$ films and their Mössbauer observations had three types of hyperfine fields corresponding to the three inequivalent Fe sites in $Fe_{16}N_2$, where the hyperfine field of Fe(2) is the highest. Recently, they obtained another Mössbauer spectrum and found that the hyperfine fields of Fe(1) and Fe(2) sites are lower than that of α-Fe, while that of Fe(3) is much higher. Sugita *et al* observed $B_s \approx 3.0$ T in the single phase $Fe_{16}N_2$ films, but the Mössbauer spectrum, like that of Kim and Takahashi, had only two types of hyperfine field.

Table 1. Hyperfine fields for inequvalent sites in $Fe_{16}N_2$ structure from the Mössbauer effect. Unit: kOe.

Reference	Sample	Fe(1)	Fe(2)	Fe(3)
Kim *et al* (1972)	Mixed phase	374	216	
Moyira *et al* (1973)	Mixed phase	302	418	325
Nakajima *et al* (1989)	Mixed phase	298	372	316
Sugita *et al* (1991)	Single phase	330	460	
Nakajima *et al* (1991)	Mixed phase	291	315	367

α-Fe: 340

Studying the effects of non-magnetic elements, such as B, C, P, Al, Si and N, on

the magnetic moment of transition metals of Fe, Co and Ni is of great importance in understanding their alloys. Mater *et al* [10] have performed augmented sphere wave (ASW) calculations on Fe_4N. The calculated magnetic moment was in good agreement with neutron data. They also discussed in detail the interactions of Fe–N atoms and found that there was no charge transfer between Fe and N atoms. Sakuma [11] performed linearized muffin-tin orbital (LMTO) calculations on Fe_3N, Fe_4N and $Fe_{16}N_2$ structures. He obtained $2.40\mu_B$ for the average magnetic moment per atom. However, this value is smaller than the experimental value, $\approx 3.0\mu_B$.

The purpose of the present paper is to investigate the electronic structure and magnetic behaviour of BCT-FeN compounds. We have used a cluster approach where the reasonable size clusters of Fe–N atoms representing the local environments for atoms of interest were treated exactly using the first-principles discrete variational method [12]. Such an approach is efficient in the study of a complicated system with low symmetry, and its success in studying impurities and defects in transition metals and their oxides is well established [13, 14]. In particular, calculations on the variation of the local magnetic moment and DOS have proved to be very satisfactory by choosing an appropriate metal cluster wherein the near-neighbour interactions are included in the cluster.

2. Theoretical model and computational procedure

Four clusters based on figure 1(*a*) were used in our calculations:

(A) Fe_{22} cluster representing the BCC pure iron with lattice constant 2.866 Å.

(B) NFe_{22} cluster with one N atom in the octahedral interstitial site representing the BCT α'-martensite structure. $a = 2.866$ Å, $c = 3.15$ Å, see figure 1(*a*).

(C) As cluster B, but the distance between two F(1) atoms is 3.88 Å, representing the $Fe_{16}N_2$ structure.

(D) Fe_15N_4 cluster shown in figure 7(*c*), representing the local environment of the Fe(3) site in $Fe_{16}N_2$.

These models are referred to as clusters A, B, C and D in the paper.

Our calculations are based on a self-consistent-field linear-combination-of-atomic-orbital molecular-orbital (SCF-LCAO-MO) method [12]. The MO eigenstates $\psi_n(r)$ are expanded in terms of symmetry orbitals $\chi_j(r)$

$$\psi_n(r) = \sum_j C_{nj}\chi_j(r). \tag{1}$$

The $\chi_j(r)$ are chosen as linear combinations of atomic orbitals centred on different atoms corresponding to the cluster point-group symmetry. The coefficients C_{nj} in equation (1) are obtained by solving the single-particle equation

$$(H - \epsilon_n)\phi_j(r) = 0. \tag{2}$$

The effective Hamiltonian for spin σ is given in atomic units as

$$H_\sigma = -\tfrac{1}{2}\nabla^2 + V_{\text{Coul}}(\rho_\sigma) + V_{\text{xc}}(\rho_\sigma). \tag{3}$$

The various terms in equations (2) and (3) carry their conventional meaning.

The remaining calculations are done by applying the local density approximation [15] to the exchange and correlation potentials. We have used the von Barth–Hedin [16] form of the spin-dependent potential for this purpose. The spin–orbit interaction has not been included in the study, and thus we neglected the orbital moment, about 0.05–0.1μ_B, which is much smaller than the spin moment for transition metals. Equation (2) is solved using the discrete variational method (DVM) where one minimizes certain error moments on a diophantine sampling grid [12]. The matrix secular equation $(\mathbf{H} - E\mathbf{S}) = 0$, where $\mathbf{H}$ and $\mathbf{S}$ are the Hamiltonian and overlap matrices, respectively, is solved by standard procedures. The cluster charge density is constructed by summing over all MOs with occupation $f_n(\epsilon)$

$$\rho_{\text{cluster}} = \sum_n f_n |\psi_n(r)|^2. \tag{4}$$

In simulating the bulk solid form as a finite cluster of atoms, each of the clusters is embedded in the effective crystal potential field constructed by placing atomic potentials at appropriate lattice sites around the cluster. The frozen core approximation was also used in all cases.

3. Results and discussions

For a cluster with inequivalent sets of atoms in different environments, it is natural that the atoms with more complete coordination shells may describe better the properties of bulk solid [14]. We first consider the pure iron cluster A, where the Fe(1) and Fe(2) sites are more suitable to represent the bulk; thus, we are mainly interested in the electronic and magnetic properties of these two sites. Fe(3) and Fe(4) are surface atoms in the cluster which are strongly influenced by surface effects.

Magnetic moments, calculated by taking the difference between Mulliken populations [17] for spin-up and spin-down electrons of 3d, 4s and 4p orbitals, and the Fe 3d charges at different sites are listed in table 2. The Fe(1) and Fe(2) atoms have moments of 2.77 and 3.65μ_B respectively, which are larger than the magnetic moment of bulk iron atoms of 2.2μ_B due to the finite cluster size effect, but these values are comparable to the central Fe moment of 2.80μ_B in the Fe_{15} cluster [14].

Table 2. Total magnetic moments and d charges at different sites for clusters A, B and C described in section 2.

	Atom numbers	Fe(1)	Fe(2)	Fe(3)	Fe(4)	N
Cluster A	22					
μ (μ_B)		2.77	3.45	3.76	3.92	
d charge		6.44	6.25	6.17	6.01	
Cluster B	23					
μ (μ_B)		2.39	3.63	3.80	3.97	−0.69
d charge		6.40	6.30	6.21	6.11	
Cluster C	23					
μ (μ_B)		2.65	3.35	3.89	3.92	−0.88
d charge		6.45	6.34	6.20	6.03	

In the DVM cluster calculations, the total density of states includes contributions from all the inequivalent sites and does not compare well with the band structure

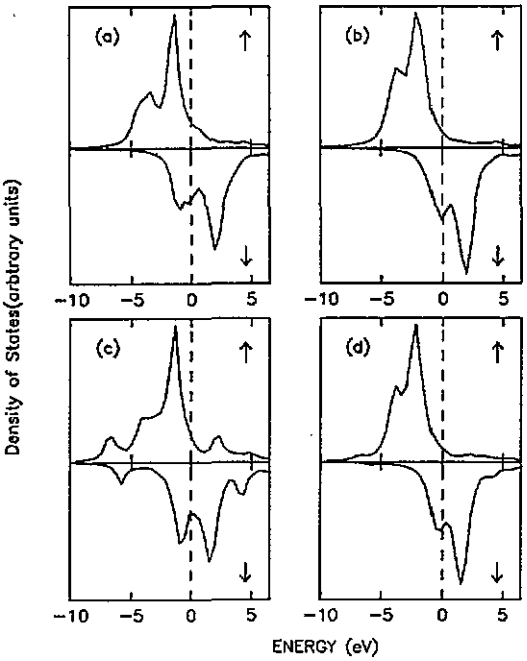

Figure 3. 3d DOS of (*a*) Fe(1) in cluster A, (*b*) Fe(2) in cluster A, (*c*) Fe(1) in cluster B, (*d*) Fe(2) in cluster B. The spin-up and spin-down bands are normalized to the same scale within each cluster.

calculations. It is more instructive to look at the partial DOS from individual atoms which were considered to be more bulk-like. The 3d DOS of Fe(1) and Fe(2) obtained by the Lorenzian broadening (0.4 eV) of the discrete electronic levels are shown in figure 3(*a*) and (*b*), which turn out to be in agreement with the DOS obtained by Moruzzi *et al* [18]. However, our 3d DOS have less fine structure because we did not include the contributions from 4s and 4p orbitals.

Next, we examine the effects of N atoms on the electronic structure and magnetic moment of the neighbouring Fe atoms. The results for cluster B, representing the α'-martensite Fe–N, are listed in table 2. It is noted that the Fe(1) magnetic moment is reduced while that of other sites increases a little; this trend is in good agreement with the Mössbauer studies on α'-martensite Fe–N [2]. It is worth pointing out that the Fe(4) atoms are hardly affected by the N atoms.

Mitsuoka *et al* [3] ascribed the magnetic moment reduction of the first-neighbour Fe atoms of N to the charge transfer from N to the Fe 3d band. However, ASW calculation on Fe_4N showed that there is no charge transfer between Fe and N. LMTO [11] and LAPW [19] studies on Fe_4N found the charge transfer from Fe to N. From table 2 we note that the 3d charges have no obvious variances with or without the N atom. Therefore the charge transfer is not observed in our Mulliken population analysis.

The 3d DOS for Fe(1) and Fe(2) and N 2p DOS of cluster B are shown in figure 3(*c*), (*d*) and figure 4, respectively. The impurity states of N 2p are obviously observed in figure 3(*c*), at about −6 eV below and 2–4 eV above the Fermi level for bonding and antibonding states, respectively. Hence the reduction of the Fe(1) magnetic moment in cluster B is due to the N 2p and Fe 3d interactions which transfer the majority 3d electrons to the minority 3d band.

It is now well recognized that the magnetic moment of transition metals depends on the overlaps of the wavefunctions of neighbouring atoms. Increasing the lattice constant will reduce the interactions of atoms and lead to the increase of the atomic

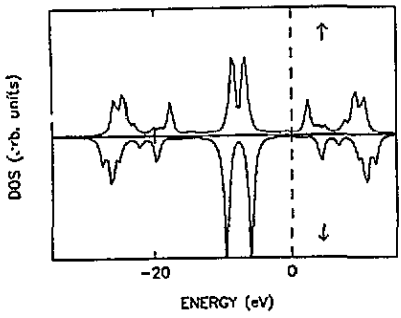

Figure 4. 2p density of states of the central N in cluster B.

magnetic moment [20]. Indirect evidence can be given here. The high spin state of γ-Fe has the magnetic moment of $2.8\mu_B$. The FCC γ-Fe structure could be achieved with an elongation of the BCC structure along the ⟨100⟩ axis to $c = \sqrt{2}a$ and rotating the reference frame by 45°. Therefore the magnetic moment increase from BCC to FCC structure is caused by the elongation of the c axis. The α'-martensite FeN is of BCT structure ($1 < c/a < \sqrt{2}$), and has a structure intermediate between BCC ($c/a = 1$) and FCC ($c/a = \sqrt{2}$) structure; its magnetic moment should be between $2.2\mu_B$ and $2.8\mu_B$.

Based on the above discussions, we note that when the N atoms enter into the interstices, the tetragonal expansion will give rise to the increase of the magnetic moment; meanwhile, the N atoms will reduce the moment of neighbouring atoms. Thus, the magnetic moment of Fe atoms in the Fe–N compound is determined by the competition of these two opposite factors.

From figure 3(*d*), we note that the Fe(2) 3d DOS has not been affected by N atoms. Moreover, due to the larger lattice constant in cluster B, the overlap between adjacent atomic orbitals is small; thus the Fe(2) d band is sharper than in cluster A. Although we could not get absolute sharpness from the cluster calculation, the relative profile could be obtained because we used the same broadening factor for all the discrete levels of the clusters. In figure 5, we show the charge density of cluster B on the (110) plane. It can be seen that the central N atom is almost completely screened by Fe(1) atoms and has no obvious bonding with Fe(2) atoms. Thus the tetragonal effect dominates over that of the N atom for Fe(2), resulting in the increase of the magnetic moment, while the interactions between N and Fe(1) atoms overwhelm the tetragonal elongation and lead to the reduction of the Fe(1) magnetic moment.

Finally we discuss the results for cluster C representing the $Fe_{16}N_2$ structure. The lattice parameters in cluster C are the same as those of the $Fe_{16}N_2$ structure proposed by Jack [9], except that the local environment of Fe(3) is not complete due to the small cluster. Thus we concentrate on the results for Fe(1) and Fe(2) sites. The calculation results for cluster C in table 2 indicate that the Fe(1) and Fe(2) magnetic moments are all reduced compared with those of the pure iron cluster A.

Nakajima [4] reported that the internal field of Fe(2) was 38% higher than that of Fe(1) atoms in the $Fe_{16}N_2$ phase formed by ion implantation on α-iron. However, in the $Fe_{16}N_2$ structure, the distance of Fe(1) from the central N (1.95 Å) is very close to that of Fe(2) from N (2.02 Å). The charge density of cluster C on the (110) plane in figure 6 shows clearly the same bonding of N with Fe(1) and Fe(2) atoms, which means that the Fe(1) and Fe(2) atoms will be equivalently affected by N atom.

It is well known that the magnetic moment and hyperfine field is determined by the local environment. Figure 7 shows the local environments of Fe(1), Fe(2) and Fe(3) sites, respectively. It can be seen from this figure that the local coordinates of

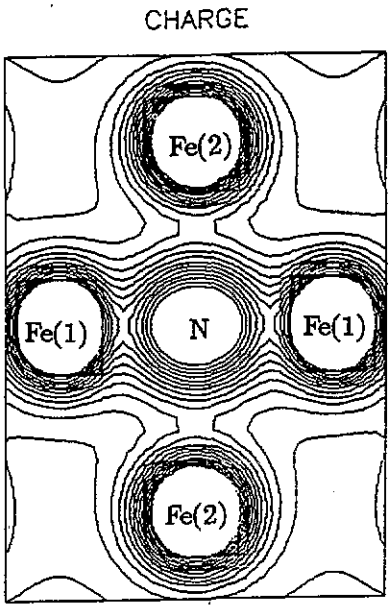

Figure 5. Charge density of cluster B (α'-martensite) on the (110) plane.

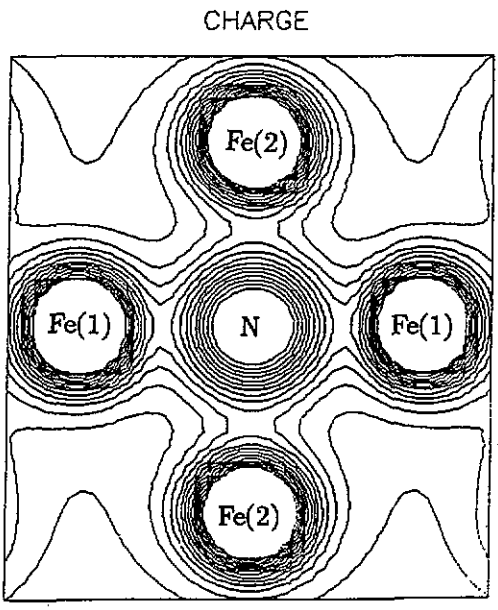

Figure 6. Charge density of cluster C (α''-martensite $Fe_{16}N_2$) on the (110) plane.

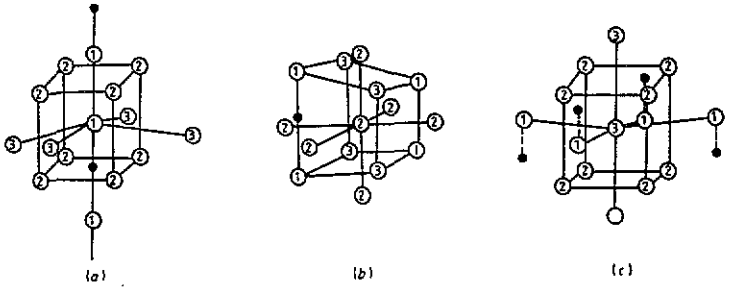

Figure 7. Local environments for the inequivalent sites of $Fe_{16}N_2$. (*a*) Fe(1), (*b*) Fe(2), (*c*) Fe(3).

Fe(1) and Fe(2) are similar when compared with that of α-Fe and have no significant differences except for a nearest-neighbour N atom. However, the local environment of Fe(3) site is quite different, due to the tetragonal elongation around Fe(3). On the other hand, there are no nearest-neighbour N atoms for the Fe(3) site. Therefore the hyperfine field of Fe(3) will increase compared with that of α-Fe, in agreement with recent experimental and theoretical studies [11].

In order to obtain the magnetic moment change of Fe(3) from that of α-Fe, we calculate the cluster $Fe_{15}N_4$ of figure 7(*c*) and find that the magnetic moment of the central atom increases by $0.3\mu_B$ from that of the Fe_{15} cluster representing the pure α-Fe. Therefore the average magnetic moments calculated by us and by Sakuma [11] are smaller than that of experiment. The origins may be due to the local density approximation and various synthesizing methods which give different results. On the other hand, the $Fe_{16}N_2$ compounds were formed in the thin film states; the

distortion of the arrangement of Fe atoms on the surface may be a reason for the high magnetization. Komuro *et al* [6] observed that the saturation magnetic flux density increased with decreasing Fe–N film thickness and suggested the existence of a large lattice spacing in the Fe–N films.

4. Conclusion

We have performed self-consistent spin polarized cluster calculations on the electronic structure and magnetic moment of martensite FeN compounds. The computational method has been widely and successfully used in studying the local magnetic properties of transition metals, where the much localized d electrons determine the electronic and magnetic structures and hence a finite cluster may be a good representation of bulk solid. However, the calculated average magnetic moment for $Fe_{16}N_2$ is smaller than that of experiment. More experimental and theoretical studies are needed to investigate the magnetic properties of α''-$Fe_{16}N_2$ compound.

We found that the addition of N atoms in α-Fe has two effects. The first is to expand the lattice parameters and the second is to reduce the magnetic moment of nearby atoms. If the former dominates the latter the average magnetic moment will increase. This is the case for N in R_2Fe_{17} (R = rare earth element) [21] and B in R_2Fe_{14} compounds [22].

Acknowledgments

The author thanks Professors Q Q Zhengand W Y Lai for fruitful discussions.

References

[1] Kim T K and Takahashi M 1972 *Appl. Phys. Lett.* **20** 492
[2] Moriya T, Sumitomo Y, Ino H, Fujita F E and Maeda Y 1973 *J. Phys. Soc. Japan* **35** 1378
[3] Mituoka K, Miyajima H, Ino H and Chikazumi S 1984 *J. Phys. Soc. Japan* **53** 238
[4] Nakajima K, Okamoto S and Okada T 1989 *J. Appl. Phys.* **65** 4357
[5] Nakajima K and Okamoto S 1989 *Appl. Phys. Lett.* **54** 286; 1990 *Appl. Phys. Lett.* **56** 92
[6] Komuro M, Kozono Y, Hanozono H and Sugita Y 1990 *J. Appl. Phys.* **67** 5126
[7] Nakajima K, Okamoto S, Takata M and Sekizawa H 1991 *J. Magn. Soc. Japan* **15** 703
[8] Sugita Y, Mituoka K, and Komuro M 1991 *J. Magn. Soc. Japan* **15** 667
[9] Jack K H 1951 *Proc. R. Soc.* A **208** 216
[10] Mater S, Mohn P, Demazeau G and Siberchicof B 1988 *J. Physique* **49** 1761
[11] Sakuma A 1991 *J. Phys. Soc. Japan* **60** 2007; 1991 *J. Magn. Magn. Mater.* **102** 127
[12] Ellis D E 1968 *Int. J. Quantum Chem.* **35** 2
Ellis D E and Painter G P 1970 *Phys. Rev.* B **2** 2887
[13] Li Z Q, Luo H L, Lai W Y, Zeng Z and Zheng Q Q 1991 *J. Magn. Magn. Mater.* **98** 47
[14] Li Z Q, Luo H L, Lai W Y and Zheng Q Q 1991 *J. Phys.: Condens. Matter* **3** 6649
[15] Kohn W and Sham L J 1965 *Phys. Rev.* **140** A 1133
[16] von Barth U and Hedin L 1972 *J. Phys. C: Solid State Phys.* **5** 1629
[17] Mulliken R S1933 *Phys. Rev.* **45** 87
[18] Moruzzi V L, Janak J F and Williams A R 1978 *Calculated Electronic Properties of Metals* (New York: Pergamon)
[19] Zhou W, Qu L J, Zhang Q M and Wang D S 1989 *Phys. Rev.* B **40** 6393
[20] Liu F, Press M R, Khanna S N and Jena P 1989 *Phys. Rev.* B **39** 6419
[21] Jaswel S S, Yelon W B, Hadjipanayis G C, Wang Y Z and Shellmer D J 1991 *Phys. Rev. Lett.* **67** 644
[22] Coehoon R 1991 *J. Magn. Magn. Mater.* **99** 55